Controlling the Bimolecular Reaction and Photodissociation of HNCO through Selective Excitation of Perturbed Vibrational States†

Ephraim Woods III,‡ H. Laine Berghout,§ Christopher M. Cheatum, and F. Fleming Crim*

Department of Chemistry, University of Wisconsin-Madison, Madison, Wisconsin 53706

Received: April 10, 2000; In Final Form: June 14, 2000

Selective reaction or photodissociation of isocyanic acid (HNCO) molecules in well-characterized vibrational eigenstates is a means of controlling their chemistry. The key to the measurements is the characterization of their vibrational states by absorption spectroscopy and the determination of their reaction efficiency by action spectroscopy. Absorption spectroscopy and theoretical calculations on states in the region of three quanta of the N−H stretching excitation ($3\nu_1$) of HNCO identify couplings between the bright N−H stretching state and states that have one or more quanta of N−C−O bending excitation. Bimolecular reaction action spectroscopy, which monitors the yield of NCO from the reaction of Cl atoms with HNCO, and photodissociation action spectroscopy, which monitors the production of ^{1}NH following $S_1 \leftarrow S_0$ excitation in HNCO, measure the relative reaction and photodissociation cross sections for the *mixed vibrational eigenstates* having rotational quantum numbers $K = 3$ and $J = 6$ and 7. The measurements and analysis show that the perturbing zero-order state is substantially *less* reactive than the bright state but has a photodissociation cross section that is much *larger* than that of the bright state. Bending excitation of N−C−O strongly influences both the reaction and photodissociation, hindering bimolecular reaction but promoting photodissociation.

I. Introduction

State-resolved measurements often reveal the details of molecular transformations such as bimolecular reaction and photodissociation. Because the stretching of chemical bonds is generally a precursor to breaking them, the vibrational state of a molecule often plays an important role in chemical reactions. Light-atom stretching excitations strongly influence the rate of endothermic H-atom abstraction reactions, as illustrated by the reactions of H,[1−5] Cl,[6] and O[7] atoms with HOD and HCN. Similarly, O−H and O−D stretching excitations alter cross sections, energy partitioning, and product branching in the photodissociation of H_2O and HOD.[8−11] In cases where the vibrational states are well-characterized, one can correlate the specific motions of the nuclei with the resulting dynamics. This understanding enables control of the outcome of reactions by a judicious choice of vibrational state, as measurements on both the reaction and photodissociation of HOD demonstrate. Because the stretching vibrations of HOD are relatively unperturbed, selective vibrational excitation places energy directly into a motion that becomes the reaction coordinate. For instance, excitation of the O−H stretch in HOD promotes breakage of that bond in bimolecular reactions[1−5] and in photodissociation.[9−11] The situation is more complex in larger molecules where the vibrational eigenstates are a mixture of many zero-order states, and the effects of motions that are normal to the reaction coordinate are more subtle.

We have investigated the behavior of strongly mixed eigenstates in the bimolecular reaction and photodissociation of isocyanic acid (HNCO) excited in the region of three quanta of the N−H stretching vibration ($3\nu_1$). Although HNCO has only four atoms, both its vibrational spectrum[12−16] and its photodissociation[17−20] dynamics are interesting and complex. HNCO is a near-prolate symmetric top ($\kappa = 0.9997$), and the quantum numbers J and *K* describe the total angular momentum and the projection of the total angular momentum onto the principle inertial axis, respectively. Absorption spectroscopy of the $3\nu_1$ state reveals several vibrational couplings throughout the spectrum, most notably a moderately strong two-state interaction for the $K = 3$, $J = 4-10$ angular momentum states.[14] Because these pairs of perturbed eigenstates are well separated in energy, selective excitation of states with different amounts of the perturbing vibration is possible. Our approach is to use the information from absorption spectroscopy to characterize the mixed vibrational states and to examine the effects of selective excitation on both bimolecular reaction and photodissociation dynamics using action spectroscopy.

Action spectroscopy, which combines absorption spectroscopy with a probe of the subsequent dynamics, enables the direct comparison of cross sections for processes such as bimolecular reactions and photodissociation for individual quantum states. A comparison of the absorption spectrum and the action spectrum yields both qualitative and quantitative information about the quantum state dependence of the reaction and photodissociation dynamics. The measurements reveal the influence that the vibrational character of the states has on the efficiency of reaction and photodissociation.

II. Experimental Approach

Our methods of investigating the bimolecular reaction and photodissociation dynamics are similar to those we have used previously. For the bimolecular reaction experiments,[21] one laser prepares a specific rovibrational state of HNCO, another laser creates Cl atoms by photolysis of Cl_2, and a third laser probes

† Part of the special issue "C. Bradley Moore Festschrift".

* Author to whom correspondence should be addressed.

‡ Present address: Department of Chemistry, University of North Carolina−Chapel Hill, Chapel Hill, NC 27599.

§ Present address: Los Alamos National Laboratory, Los Alamos, NM 87544.

10.1021/jp001369d CCC: $19.00
Published on Web 08/10/2000

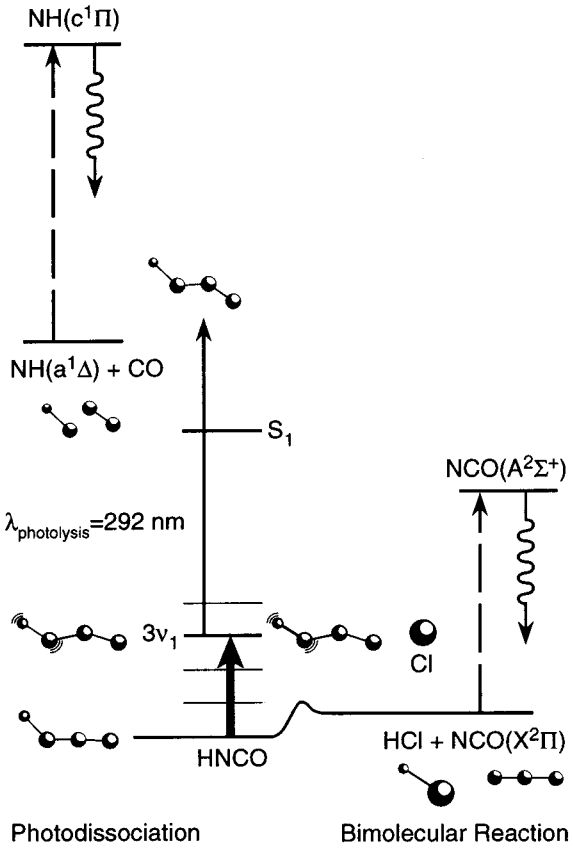

Figure 1. Energy-level diagram for the photodissociation (left) and bimolecular reaction with Cl (right) of vibrationally excited HNCO. The bold arrow indicates the excitation that prepares states in the region of three quanta of N−H stretching excitation ($3\nu_1$). The left-hand side of the diagram shows the photodissociation scheme in which we excite the vibrationally excited molecule to the S_1 electronic state from which it dissociates to form ^{1}NH, which we detect by laser-induced fluorescence. The right-hand side shows the bimolecular reaction scheme in which the vibrationally excited molecules react with Cl atoms to form NCO, which we also detect by laser-induced fluorescence.

the NCO product of the subsequent reaction by laser-induced fluorescence (LIF). In the vibrationally mediated photodissociation experiments,[18] one laser again prepares a specific rovibrational state of HNCO, and another laser promotes the molecule to the S_1 excited electronic state. Molecules in the excited state dissociate to form ^{1}NH and CO, and a third laser probes the ^{1}NH fragment using LIF. Figure 1 illustrates these experimental schemes in which we either photodissociate the vibrationally excited molecule, as shown on the left, or react it, as shown on the right. To record action spectra in each experiment, we fix the wavelength of the probe laser to monitor a specific product state of either ^{1}NH or NCO and scan the vibrational overtone excitation laser through the rovibrational spectrum. We observe a signal in the action spectrum when the vibrational overtone excitation laser is resonant with an overtone transition *and* the prepared molecule reacts or dissociates to form the product in the monitored quantum state.

We have described the details of the experimental arrangement for both bimolecular[21] reaction and photodissociation[18] experiments previously and only outline the procedure here. In the bimolecular reaction studies, the reagent gases, HNCO and Cl_2, enter a low-pressure reaction cell through separate ports at a constant flow rate. We maintain the cell at 200 mTorr total pressure during the experiment, with each gas accounting for one-half of the concentration. Direct vibrational overtone excitation with 15-mJ pulses from a Nd:YAG laser-pumped dye laser prepares vibrationally excited states of HNCO. Tripling the residual fundamental light (1.06 μm) from this Nd:YAG laser generates 7-mJ pulses of 355-nm light that photodissociate Cl_2 to produce Cl atoms. After a delay of 500 ns, <500-μJ pulses of light near 440 nm from another Nd:YAG laser-pumped dye laser probe the NCO product by partially saturated laser-induced fluorescence on the A $^2\Sigma^+ \leftarrow$ X $^2\Pi$ band. A photomultiplier tube collects the fluorescence through *f*/1 optics, and a bandpass filter discriminates against scattered photolysis light.

The vibrational preparation scheme is the same in the photolysis experiment, but we photodissociate, rather than react, the vibrationally excited molecule. Less than 20 ns after the vibrational excitation, a 5-mJ, 292-nm pulse from a frequency-doubled Nd:YAG laser-pumped dye laser dissociates vibrationally excited HNCO molecules to form ^{1}NH and CO fragments. (The two lower-energy decomposition channels, producing ^{3}NH + CO and NCO + H, are minor contributors at the energies we use.) After a 1-μs delay, a 50-μJ pulse of 326-nm light from another frequency-doubled Nd:YAG laser-pumped dye laser detects the ^{1}NH product by LIF on the c$^1\Pi \leftarrow$ a$^1\Delta$ band. We detect the ^{1}NH product in order to obtain the best signal-to-noise ratio, but the features in the action spectrum do not depend on the identity of the detected product. The total excitation energy of 44 250 cm^{-1} exceeds the ^{1}NH + CO threshold[22] by 1540 cm^{-1} and leaves HNCO in a region of the excited-state potential energy surface where ^{1}NH is the dominant decomposition product.[20,23,24] Our initial vibrational excitation primarily alters the excitation efficiency through the Franck−Condon factor, rather than influencing the dissociation dynamics. We record the absorption spectrum using photoacoustic spectroscopy in concert with the action spectra in both the bimolecular reaction and photodissociation experiments. A portion of the overtone excitation laser beam passes through a photoacoustic cell filled with about 1 Torr of HNCO gas, and we record the absorption and action spectra simultaneously in order to reduce errors arising from intensity fluctuations in the vibrational overtone excitation laser.

III. Absorption and Action Spectroscopy of Mixed Eigenstates

The rovibrational eigenstates that we excite in the region of $3\nu_1$ are mixtures of vibrational states, and a simple two-state model can describe the intensities of transitions to the perturbed eigenstates in the absorption and action spectra. We write the mixed eigenstate prepared in the vibrational overtone excitation as a linear combination of two zero-order states.

$$|n\rangle = C_s^n|s\rangle + C_l^n|l\rangle \tag{1}$$

Because the bright state $|s\rangle$ carries the oscillator strength for the optical transition and the dark state $|l\rangle$ has no oscillator strength in this model, the intensities of the transitions to each of the eigenstates in the absorption spectrum are proportional to $|C_s^n|^2$. Thus, the mixing coefficients are

$$|C_s^{1,2}|^2 = A_{1,2}/(A_1 + A_2) \tag{2}$$

where A_1 and A_2 are the respective areas of a pair of perturbed eigenstates arising from the same pair of zero-order states. In our experiments, the bright zero-order state is the state with three quanta of N−H stretching excitation ($3\nu_1$) to a very good approximation,[25] and the dark zero-order state is typically a state with one or more quanta of N−H stretching vibration replaced by other stretching and bending vibrations.

TABLE 1: Best-Fit Spectroscopic Parameters[a] for the Bright and Dark Zero-Order States

	energy $F(J=0, K=3)$	rotational constant B	distortion constant D_J	matrix element $\|V\|$
bright state, $\|s\rangle$	$10\,347.24 \pm 0.02$	0.3645 ± 0.0001	$\sim 1 \times 10^{-7}$	0.035 ± 0.003
dark state, $\|l\rangle$	$10\,346.76 \pm 0.02$	0.3698 ± 0.0002	$\sim 1 \times 10^{-7}$	

[a] Values are in cm^{-1}.

The intensities of features in action spectra depend on both the vibrational excitation probability and the probability that the prepared state will produce, either through bimolecular reaction or photodissociation, the product in the state probed by the experiment. A comparison of the action spectrum to the absorption spectrum gives the relative reaction or photodissociation cross section for each state. We use the intensity of the transition in the absorption spectrum as a measure of the vibrational excitation probability and write the relative reaction or photodissociation cross section as

$$\sigma_n/\sigma_0 \propto I_{\text{action}}/I_{\text{absorption}} \tag{3}$$

where σ_0 is the cross section for an arbitrary reference state ($J = 8$, $K = 3$) for which we equate the intensities in the action and photoacoustic spectra. Having the relative cross sections for each of the eigenstates, we extract cross sections for the zero-order states that constitute the eigenstate. If we can identify the contributing zero-order states, we can then connect their reaction or photodissociation cross sections with the dynamics arising from specific nuclear motions.

Our approach to analyzing the measurements is similar for both the bimolecular reaction and photodissociation experiments.[21] If $\boldsymbol{P}$ is the operator that carries the reactants out of the initial eigenstate $|n\rangle$ to form products in the final state $|f\rangle$, then the bimolecular reaction cross section is

$$\sigma_{fn}^{\text{R}} \propto |\langle f|\boldsymbol{P}|n\rangle|^2 = |C_s^n\langle f|\boldsymbol{P}|s\rangle + C_l^n\langle f|\boldsymbol{P}|l\rangle|^2 = |C_s^n|^2|P_{fs}|^2 + |C_l^n|^2|P_{fl}|^2 + 2C_s^nC_l^n|P_{fs}P_{fl}| \tag{4}$$

where we have used the expansion of $|n\rangle$ in the zero-order states (eq 1). The matrix elements P_{fs} and P_{fl} describe the reaction of each of the zero-order states. We take the coefficients of the expansion to be real, but, because their signs depend on the details of the state mixing, the cross term can either increase or decrease the reaction cross section.

The ratio of the relative reaction cross sections of two eigenstates, $|1\rangle$ and $|2\rangle$, that contain different amounts of the same bright and dark zero-order states is

$$\sigma_{f1}^{\text{R}}/\sigma_{f2}^{\text{R}} = (|C_s^1|^2 + |C_l^1|^2\Omega^2 + 2C_s^1C_l^1\Omega)/(|C_s^2|^2 + |C_l^2|^2\Omega^2 + 2C_s^2C_l^2\Omega) \tag{5}$$

where $\Omega = |P_{fl}/P_{fs}|$ is the ratio of the reaction matrix element of the dark zero-order state to that of the bright zero-order state. Because we know the magnitude of the expansion coefficients from the absorption spectrum and the relative reaction cross section from the action spectrum, we can extract Ω and, thus, the relative reactivity of the two states.[21] The areas of the features in the absorption spectrum (eq 2) provide the coefficients of the expansion, $|C_s^n|$ and $|C_l^n|$, and the ratio of intensities in the action and absorption spectra (eq 3) gives the relative reaction cross sections of the mixed eigenstates, σ_{fn}^{R}. Although our absorption spectrum does not give the signs of the coefficients in eq 5, we do know that the cross terms have opposite signs, as the two linear combinations must be out of phase. After obtaining the relative reaction cross section ($\sigma_n^{\text{R}}/\sigma_0^{\text{R}}$) for each eigenstate from the action and photoacoustic spectra, we solve eq 5 with an arbitrary choice of phase to obtain one positive and one negative root. The other choice of phase leads to the same roots with opposite signs. We select the appropriate solution by requiring that the bright state be more reactive than the dark state, $|\Omega| < 1$.

Extending our approach to include the photolysis action spectrum is straightforward. If the electronic and vibrational degrees of freedom are separable, then the initial and final states are each products of electronic and vibrational wave functions. The relevant operator for the photolysis is the electric dipole moment operator, μ, which promotes the excited vibrational state to the dissociative electronically excited state $|f\rangle$. (We observe the product to which the dissociative state $|f\rangle$ correlates. The photolysis cross section is that for producing products in the probed fragment quantum state.[26,27]) Factoring out the electronic transition moment, μ_{fn}, gives the photolysis cross section as

$$\sigma_{fn}^{\text{P}} \propto |\langle f|\mu|n\rangle|^2 = |\mu_{fn}|^2|C_s^n\langle f|s\rangle + C_l^n\langle f|l\rangle|^2 = |\mu_{fn}|^2(|C_s^n|^2|\langle f|s\rangle|^2 + |C_l^n|^2|\langle f|l\rangle|^2 + 2C_s^nC_l^n|\langle f|s\rangle\langle f|l\rangle|) \tag{6}$$

This expression is analogous to eq 4, but the Franck Condon factors, $\langle f|s\rangle$ and $\langle f|l\rangle$, play the role of the reaction probability matrix elements. Using this equation, we calculate the ratio of Franck Condon factors for the dark and bright states, $|\langle f|l\rangle/\langle f|s\rangle|$, just as we did for the relative reaction cross section.

The derivation of these relationships relies on the assumption that the action spectra are independent of the monitored state of the product, which requires that the identity of the initially prepared vibrational state affect only the total reaction or photodissociation cross section and not the distribution of the products among their quantum states. For the bimolecular reaction experiment, we have previously demonstrated the independence of the action spectrum from the final state of the NCO product.[21] In general, when one of the zero-order states is very unreactive, as we show below to be the case for both reaction and photodissociation of HNCO, the product state distribution is nearly the same for reaction from either initial state.

IV. Results and Analysis

A. Absorption Spectroscopy. We model the absorption spectrum of the $K = 3$ subband of $3\nu_1$ by simulating the unperturbed features in the spectrum to obtain the spectroscopic constants for the bright zero-order state $|s\rangle$ given in Table 1. Although there are high-order perturbations for some rotational states throughout the spectrum, we treat only the largest perturbation for the states $J = 5-12$. Because we model the perturbations as a two-state anharmonic interaction, the magnitude of the mixing coefficients is the ratio of the areas of the features in the spectrum, as described above. We can directly calculate the coupling constant for the two states from the measured line positions and intensities, but additional small perturbations and spectral congestion from $K = 2$ transitions limit our confidence in such a calculation. Instead, we model the spectrum using the known bright-state parameters and treat

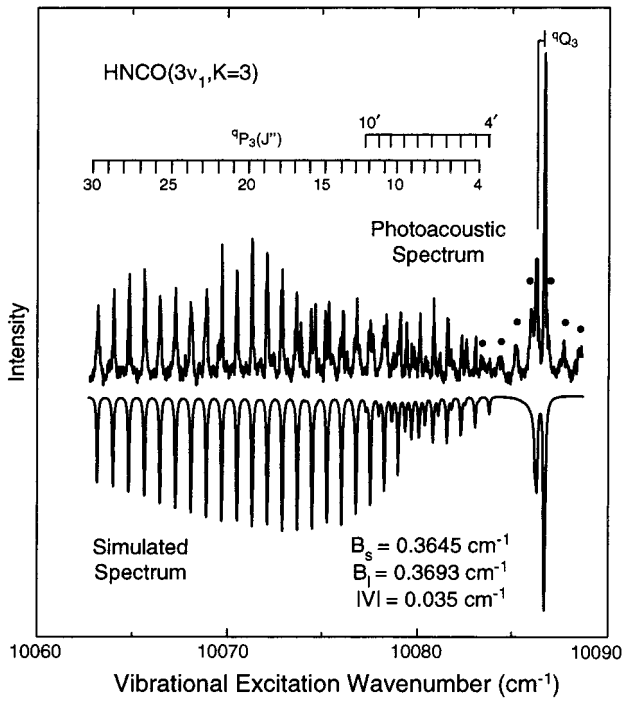

Figure 2. Measured and simulated photoacoustic absorption spectra for HNCO ($3\nu_1$, $K = 3$). The solid dots mark $K = 2$ transitions.

the coupling constant and spectroscopic constants for the dark state as adjustable parameters.

We compare the simulated spectrum to the experimental spectrum and iteratively adjust the constants to fit the measurement, obtaining the values for the dark state $|l\rangle$ given in Table 1. The rotational constant and the term value for the perturbing state are $B_l = 0.369\,8(2)$ cm^{-1} and $F(J = 0, K{=}3) = 10\,346.76(2)$ cm^{-1}, and the coupling constant between the dark and bright state is $|V| = 0.035(3)$ cm^{-1}. Figure 2 compares a portion of our observed absorption spectrum with a simulation using the best-fit parameters. There are several small features that arise from $K = 2$ transitions marked with solid circles. There are also additional interactions for states with J between 9 and 18 that double some transitions (most notably $J = 15$, 16, and 17) and give anomalous intensities. We do not treat these small couplings as they have a negligible impact on the coupling constant and dark-state rotational constant. Although the agreement between the experiment and simulation is very good throughout, it is best for J between 4 and 8 where there are only two interacting states. Because transitions from $J = 6$ and 7 have the least interference from $K = 2$ transitions or other perturbations, we analyze their reaction and photodissociation cross sections.

B. Action Spectroscopy. A previous paper describes the bimolecular reaction dynamics of HNCO ($3\nu_1$) in detail.[21] Here, we focus only on the relative reactivity of the states $J = 6$ and 7 of the $K = 3$ subband of $3\nu_1$. The middle trace in Figure 3 shows the bimolecular reaction action spectrum. For comparison, the bottom trace shows the photoacoustic (absorption) spectrum. The less-intense member of each pair of transitions for $J = 6$ and $J = 7$ in the absorption spectrum becomes even less intense in the action spectrum. We use the two-state model to determine the relative reactivities of the zero-order states shown in Table 2. Our analysis shows that the dark zero-order state is substantially *less* reactive than the bright state, with the ratio of the matrix elements for the dark and bright states being about 0.1. The solid features above spectra are portions of the spectra calculated using the spectroscopic parameters from Table 1 along with the relative reactivities and mixing coefficients from Table 2.

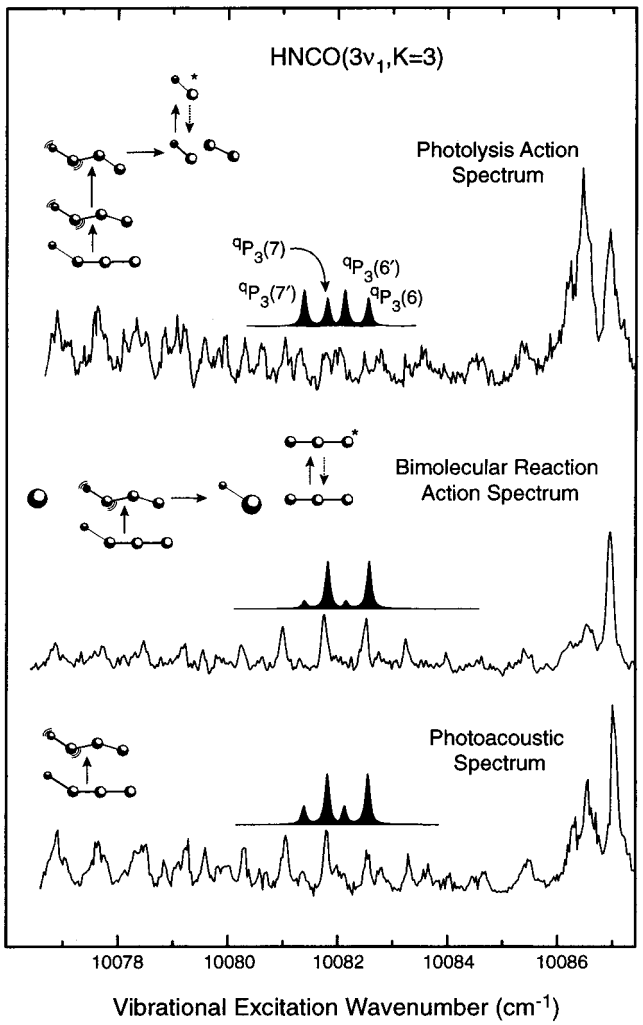

Figure 3. Action and absorption spectra for HNCO ($3\nu_1$, $K = 3$) in the region of $J = 6$ and 7. The shaded peaks are simulations using the results of the two-state model for the relative reactivities and Franck−Condon factors of the zero-order states.

TABLE 2: Bright State Content ($|C_s^n|^2$), Relative Reaction Cross Sections (σ_n^R/σ_0^R) and Matrix Elements $|P_{fl}/P_{fs}|$, and Relative Photolysis Cross Sections (σ_n^P/σ_0^P) and Franck−Condon Factors $|\langle f|l\rangle/\langle f|s\rangle|$ for HNCO ($3\nu_1$, J, $K = 3$)

		bimolecular reaction		photolysis	
J	$\lvert C_s^n\rvert^2$	σ_n^R/σ_0^R	$\lvert P_{fl}/P_{fs}\rvert$	σ_n^P/σ_0^P	$\lvert\langle f\lvert l\rangle/\langle f\lvert s\rangle\rvert$
6	0.74 ± 0.05	0.72 ± 0.05	0.13 ± 0.1	0.40 ± 0.1	12 ± 5
6′	0.26 ± 0.05	0.44 ± 0.1		1.67 ± 0.1	
7	0.71 ± 0.05	0.72 ± 0.05	0.07 ± 0.1	0.41 ± 0.1	15 ± 5
7′	0.29 ± 0.05	0.40 ± 0.1		1.33 ± 0.1	

A similar two-state analysis of the vibrationally mediated photodissociation action spectrum, shown in the top trace of Figure 3, allows us to extract the relative Franck−Condon factors for the bright and dark states. In this case, for the same pairs of perturbed eigenstates, the less-intense feature in the absorption spectrum is more intense in the action spectrum. The measured Franck−Condon factor ratio is about 13, indicating that the dark zero-order state has a larger overlap integral with vibrations in the electronically excited state than does the bright zero-order state. Thus, the intensities in the photodissociation action spectrum differ substantially from those in the absorption or bimolecular reaction action spectra.

TABLE 3: Possible Perturbing States, Energy Separation ΔE, and Coupling Matrix Elements $|V|$ for HNCO ($3\nu_1$)

order ($\Delta\nu$)	state	ΔE (cm^{-1})	$\lvert V\rvert$ (cm^{-1})
	3rd- and 4th-order couplings, $\Delta E < 300$ cm^{-1}		
4	$2\nu_1+2\nu_2+\nu_4$	214 ± 40	1.2
4	$2\nu_1+\nu_2+2\nu_5$	184 ± 3	8.7
4	$2\nu_1+2\nu_3+\nu_5$	15 ± 11	0.061
3	$2\nu_1+\nu_2+\nu_4$	-133 ± 41	19.2
	5th- and 6th-order couplings, $\Delta E < 50$ cm^{-1}		
6	$2\nu_1+4\nu_4+\nu_5$	103 ± 106	0.044ϕ[a]
6	$2\nu_1+5\nu_4$	59 ± 135	0.020ϕ
6	$2\nu_1+3\nu_5+2\nu_6$	40 ± 1	0.062ϕ
5	$2\nu_1+\nu_3+\nu_4+2\nu_5$	38 ± 30	0.216ϕ
6	$\nu_1+2\nu_2+\nu_3+\nu_4$	29 ± 48	0.108ϕ
6	$2\nu_1+3\nu_4+2\nu_5$	24 ± 20	0.062ϕ
6	$2\nu_1+2\nu_4+3\nu_5$	-4 ± 48	0.062ϕ

[a] ϕ is the fifth- or sixth-order force constant that mixes the zero-order states.

V. Discussion

Analysis of the absorption spectrum and theoretical calculations help identify the vibrational character of the dark zero-order state. Table 3 lists all of the zero-order states lying within 300 cm^{-1} of $3\nu_1$ that have a third- or fourth-order coupling with it, as well as those lying within 50 cm^{-1} that have a fifth- or sixth-order coupling.[15,16] Using anharmonic force constants from the ab initio calculations of East, Johnson, and Allen,[28] we obtain coupling matrix elements for each of the third- and fourth-order perturbations but can only calculate relative values for the higher-order interactions.[16] Clearly, there are several possible perturbers nearby in energy. As the table shows, the perturbing state is likely to have two quanta of N−H stretching excitation (ν_1) and at least one quantum of N−C−O bending excitation (ν_4 or ν_5) in combination with other vibrations. The rotational constant $B_l = 0.3698$ cm^{-1} is consistent with the dark state containing bending excitation that decreases the moment of inertia along the pseudo-symmetry axis of the molecule. These observations are the key for understanding the action spectra.

The reaction and photolysis action spectra show that the composition of the vibrational eigenstate strongly influences the reaction and photodissociation dynamics. In the case of the bimolecular reaction, the perturbing zero-order state is much less reactive than the pure N−H stretching zero-order state. The observed reactivity seems surprisingly small, as it is likely that this zero-order state has two quanta of N−H stretch, which is twice the energy required to pass over the reaction barrier.[21] For the reaction of H atoms with vibrationally excited HOD, the cross section drops by a factor of 2 between $4\nu_{OH}$ and $3\nu_{OH}$, states that have available energies similar to those for the states $3\nu_{NH}$ and $2\nu_{NH}$ in HNCO. This comparison suggests that the dark zero-order state with one quantum of N−H stretching vibration replaced by other vibrations should be about *half* as reactive as the state containing three quanta of stretching excitation, in contradiction to our observation that this state is nearly unreactive. There is sufficient excitation in the state to promote the hydrogen-abstraction reaction, but ab initio calculations show that the N−C−O bending excitation changes the interaction potential to divert reactive flux away from the abstraction channel.[21] This result implies that only states that are primarily N−H stretch will react efficiently, as the dark zero-order state not only dilutes the bright-state character but actually *hinders* the abstraction reaction. For the pairs of nearly isoenergetic eigenstates studied here, the reaction cross sections for the brighter and darker eigenstates differ from each other by about a factor of 2, and both are smaller than that of the unmixed state.[21]

The results of the photodissociation experiment stand in stark contrast. The perturbing zero-order state is much *more* efficiently photodissociated than the pure N−H stretching zero-order state. Because the N−H bond length in the S_1 state of HNCO is similar to that for the ground state, excitation of the N−H bond in the ground state does not improve the Franck−Condon factor for the $S_1 \leftarrow S_0$ transition. However, because N−C−O, which is linear in the ground state, is bent in the electronically excited state, N−C−O bending excitation significantly improves the excitation probability. The effect is so drastic that, for HNCO, vibrationally mediated photodissociation *relies* on the states being mixed, and Berghout et al. have exploited this behavior to study the electronic origin of the S_1 excited state of HNCO.[29]

The relatively weak interaction between zero-order states produces perturbed eigenstates that have substantially different dynamics when prepared individually. In the bimolecular reaction, only states that have a large component of the $3\nu_1$ (N−H stretching) vibration are able to react, but in the photodissociation, only the strongly mixed states, whose bending character gives them large Franck−Condon factors with the electronically excited state, dissociate efficiently. Even though the eigenstates are mixed, we can control their chemistry by selecting a subsequent interaction, such as bimolecular reaction or photodissociation, that operates differently on the components of the eigenstate.

VI. Conclusion

We alter the bimolecular reaction and photodissociation dynamics of HNCO by preparing states with different vibrational character. Absorption spectroscopy and theoretical analysis of mixed states in the region of the $3\nu_1$ vibration suggests that the bright N−H stretch is coupled to a state with only two quanta of N−H stretch and one or more quanta of N−C−O bending vibration. The resulting eigenstates have different bimolecular reaction and photodissociation cross sections, and their selective excitation controls the rate of reaction or photodissociation in each case. A two-state model, which uses the intensities of features in the action and absorption spectra, extracts the relative bimolecular reaction and photodissociation cross sections for the zero-order states that compose the eigenstates. We find that the perturbing vibrational state has a *smaller* bimolecular reaction probability than the bright state but, in contrast, has a *larger* photodissociation probability. Bending excitation of the N−C−O moiety is critical in both cases, altering the interaction potential between the Cl atom and the HNCO molecule to suppress the bimolecular reaction and enhancing the Franck−Condon factor for the $S_1 \leftarrow S_0$ excitation that dissociates the molecule.

Acknowledgment. We are grateful to the Division of Chemical Sciences of the Office of Basic Energy Sciences of the Department of Energy for support of our studies of vibrationally mediated photodissociation and to the National Science Foundation for support of our work on bimolecular reaction of vibrationally excited molecules.

References and Notes

(1) Sinha, A.; Hsiao, M. C.; Crim, F. F. *J. Chem. Phys.* **1990**, *92*, 6333−6335.

(2) Sinha, A.; Hsiao, M. C.; Crim, F. F. *J. Chem. Phys.* **1991**, *94*, 4928−4935.

(3) Thoemke, J. D.; Pfeiffer, J. M.; Metz, R. B.; Crim, F. F. *J. Phys. Chem.* **1995**, *99*, 13748−13754.

(4) Metz, R. B.; Thoemke, J. D.; Pfeiffer, J. M.; Crim, F. F. *J. Chem. Phys.* **1993**, *99*, 1744−1751.

(5) Bronikowski, M. J.; Simpson, W. R.; Girard, B.; Zare, R. N. *J. Chem. Phys.* **1991**, *95*, 8647−8648. Bronikowski, M. J.; Simpson, W. R.; Zare, R. N. *J. Phys. Chem.* **1993**, *97*, 2204−2208. Bronikowski, M. J.; Simpson, W. R.; Zare, R. N. *J. Phys. Chem.* **1993**, *97*, 2194−2203.

(6) Pfeiffer, J. M.; Metz, R. B.; Thoemke, J. D.; Woods, E.; Crim, F. F. *J. Chem. Phys.* **1996**, *104*, 4490−4501.

(7) Pfeiffer, J. M.; Woods, E.; Metz, R. B.; Crim, F. F. *J. Chem. Phys.*, manuscript submitted.

(8) Andresen, P.; Beushausen, V.; Häusler, D.; Lülf, H. W.; Rothe, E. W. *J. Chem. Phys.* **1985**, *83*, 1429. Häusler, D.; Andresen, P.; Schinke, R. *J. Chem. Phys.* **1987**, *87*, 3949. Engel, V.; Staemmler, V.; Vander Wal, R. L.; Crim, F. F.; Sension, R. J.; Hudson, B. J.; Andresen, P.; Hennig, S.; Weide, K.; Schinke, R. *J. Phys. Chem.* **1992**, *96*, 3201−3213.

(9) Vander Wal, R. L.; Scott, J. L.; Crim, F. F. *J. Chem. Phys.* **1990**, *92*, 803−805.

(10) Vander Wal, R. L.; Scott, J. L.; Crim, F. F. *J. Chem. Phys.* **1991**, *94*, 1859−1867. Vander Wal, R. L.; Scott, J. L.; Crim, F. F.; Weide, K.; Schinke, R. *J. Chem. Phys.* **1991**, *94*, 3548−3555.

(11) Bar, I.; Cohen, Y.; David, D.; Arusi-Parpar, T.; Rosenwaks, S.; Valentini, J. J. *J. Chem. Phys.* **1991**, *95*, 3341. Cohen, Y.; Bar, I.; Rosenwaks, S. *J. Chem. Phys.* **1995**, *102*, 3612−3616. David, D.; Strugano, A.; Bar, I.; Rosenwaks, S. *J. Chem. Phys.* **1993**, *98*, 409.

(12) Brown, S. S.; Berghout, H. L.; Crim, F. F. *J. Chem. Phys.* **1997**, *106*, 5805−5815.

(13) Brown, S. S.; Berghout, H. L.; Crim, F. F. *J. Chem. Phys.* **1997**, *107*, 9764−9771.

(14) Carlotti, M.; Lonardo, G. D.; Galloni, G.; Trombetti, A. *J. Mol. Spectrosc.* **1976**, *62*, 192−200.

(15) Coffey, M. J. Ph.D. Thesis, University of Wisconsin−Madison, Madison, WI, 1997.

(16) Coffey, M. J.; Berghout, H. L.; Woods, E.; Crim, F. F. *J. Chem. Phys.* **1999**, *110*, 10850−10862.

(17) Sanov, A.; Drozgeorget, T.; Zyrianov, M.; Reisler, H. *J. Chem. Phys.* **1997**, *106*, 7013−7022.

(18) Berghout, H. L.; Brown, S. S.; Delgado, R.; Crim, F. F. *J. Chem. Phys.* **1998**, *109*, 2257−2263.

(19) DrozGeorget, T.; Zyrianov, M.; Sanov, A.; Reisler, H. *Ber. Bunsen-Ges.* **1997**, *101*, 469−477.

(20) DrozGeorget, T.; Zyrianov, M.; Reisler, H.; Chandler, D. W. *Chem. Phys. Lett.* **1997**, *276*, 316−324.

(21) Woods, E.; Cheatum, C. M.; Crim, F. F. *J. Chem. Phys.* **1999**, *111*, 5829−5837.

(22) Brown, S. S.; Berghout, H. L.; Crim, F. F. *J. Chem. Phys.* **1996**, *105*, 8103−8110. Zyrianov, M.; DrozGeorget, T.; Sanov, A.; Reisler, H. *J. Chem. Phys.* **1996**, *105*, 8111−8116.

(23) Berghout, H. L. Ph.D. Thesis, University of Wisconsin−Madison, Madison, WI, 1998.

(24) Berghout, H. L.; Hsieh, S.; Crim, F. F., manuscript in preparation.

(25) Our earlier measurements of photolysis action spectra (ref 16) of molecules cooled in an expansion show a second-order coupling of about 18 cm^{-1} between the N−H stretching state $3\nu_1$ and a combination state $2\nu_1+\nu_2+\nu_4$ lying 174 cm^{-1} away and containing N−H stretching along with N−C−O asymmetric stretching (ν_2) and H−N−C bending (ν_4). Therefore, the state we designate as the bright state has a small component of the $2\nu_1+\nu_2+\nu_4$ vibration.

(26) Crim, F. F. *Annu. Rev. Phys. Chem.* **1993**, *44*, 397.

(27) Schinke, R. *Photodissociation Dynamics*; Cambridge University Press: Cambridge, U.K., 1993.

(28) East, A. L. L.; Johnson, C. S.; Allen, W. D. *J. Chem. Phys.* **1993**, *98*, 1299−1328.

(29) Berghout, H. L.; Crim, F. F.; Zyrianov, M; Reisler, H. *J. Chem. Phys.* **2000**, *112*, 6678−6688.